Composites Part C: Open Access 4 (2021) 100102

Contents lists available at ScienceDirect

Composites Part C: Open Access

journal homepage: www.elsevier.com/locate/jcomc

On the stochastic first-ply failure analysis of laminated composite plates under in-plane tensile loading

James R. Martinez, Peter L. Bishay*

Department of Mechanical Engineering, California State University, Northridge, 18111 Nordhoff St, Northridge, CA 91330, USA

ARTICLE INFO

Keywords:
Laminates
Mechanics of composites
Fiber-reinforced
Statistical properties/methods

ABSTRACT

This paper highlights the amount of risk taken when a deterministic approach is used in designing composite structures without consideration of stochastic effects. The study treats all material and geometric parameters of the composite laminated plates under investigation as stochastic. Monte Carlo simulation is employed to investigate the stochastic effects of material properties, ply thickness, and ply orientation on the failure of laminated composite plates under static loads. Classical lamination theory is used to calculate the strength ratios using maximum stress, Tsai-Hill, and Tsai-Wu failure criteria for plates of three different materials in various stacking sequences. Variation in the failure ply distributions are shown to increase with coefficient of variation of the input variables. A positive linear trend between the coefficients of variation of the strength ratio and input variables is found, whose slope increases as randomness is considered for more input variables. Probability of failure and failure ply distributions are shown to be heavily dependent on the combination of laminate stacking sequence, material, and failure probability. In particular, while the empirical failure probability for cross-ply laminates is highest for the ply predicted by a deterministic analysis, this probability decreases rapidly with increasing variation in input parameters. Further, the failure of unexpected plies for cross-ply laminates is shown to be related to the stiffness ratios of the plies. The general significance of considering ply thickness and ultimate strength as random variables is also demonstrated, as well as the significance of randomness in ply orientation for balanced and angle ply laminates.

1. Introduction

Laminated composite materials are prevalent in many industries for their high strength-to-weight ratios and flexibility in design. The continuous advancement and research conducted into their mechanical behavior and manufacturing has resulted in the increasing usage of such materials in various applications. Their ubiquity, especially in aerospace and aeronautical engineering, requires designers to have a thorough understanding of their mechanical behavior. However, due to the uncertainty introduced during manufacturing the composite plies and the laminated structures, a purely deterministic study can potentially be non-conservative and insufficient. Minute variations in the physical characteristics of a single ply can have disproportionally significant effects on the ultimate strength and reliability of the laminated composite structure.

Many variations of deterministic first-ply failure analyses have been performed for numerous cases. Ramtekkar et al. [1] developed a 3D layer-wise mixed finite element model to study composite laminated plates, which was also extended to the analysis of laminated composite cylindrical panels by Rattanawangcharoen [2]. Prusty et al. [3] developed a method for predicting the failure load on laminated composite stiffened panels under various loading conditions using a modified shell analysis approach. The first-ply failure of laminated panels under transverse loading was also studied for both shallow and deep shells by Prusty et al. [4] using first order shear deformation theory and the finite element method. Pal and Ray [5] went beyond the first-ply failure and studied the progressive failure analysis of composite laminates under transverse loads to determine the ultimate strength of the entire laminate using shear deformation theory and the finite element method.

Experimental data on the mechanical properties of unidirectional glass/polyester showed a coefficient of variation (CV) ranging between 10% to 20% for elastic and shear moduli as well as the material strengths, with variation as high as 24.90% [6]. In unidirectional carbon fiber-reinforced polymers (CFRP), experimental data showed variation as high as 13.1% for tensile strengths [7], with less variation in other material properties. More recent research [8] has shown that, while the elastic properties of carbon fiber/epoxy composites possess a CV of around 5%, the CV of the mechanical strength still ranges from 10% to

* Corresponding author.
E-mail address: peter.bishay@csun.edu (P.L. Bishay).

https://doi.org/10.1016/j.jcomc.2020.100102
Received 19 October 2020; Received in revised form 22 December 2020; Accepted 28 December 2020

20% [9,10]. Uncertainties in material properties obviously lead to uncertainties in failure loads, failure plies and/or failure modes, whether the composite, or hybrid composite, laminates are loaded in-plane or out-of-plane [11–13].

There have been numerous studies on the effect of randomness of material properties on composite plate mechanics. Analytical and computational models were used to analyze composite structures under various types of static and dynamic loads. For example, Salim et al. [14] investigated the response of composite plates subjected to static loads when considering only material properties as random. By solving the potential energy equation using Navier's method and validating their results with Monte Carlo simulation, they demonstrated a linear relationship between plate displacements and increasing material property variation. Lin et al. [15] evaluated both buckling and first-ply failure probabilities considering randomness in ply angle and thickness in addition to material properties. Using the stochastic finite element method (SFEM), validated with a Monte Carlo simulation, they found that ply thickness has a significant effect on laminate strength and reliability. However, randomness of lamina strength was not considered in their research. In 2000, Wu et al. [16] used the Monte Carlo approach to generate different strengths of composite lamina. The generated strengths were then used to compute the first-ply failure of composite laminates based on Tsai-Hill or Tsai-Wu criteria. Onkar et al. [17] also used SFEM to analyze first-ply failure of composite laminates with various boundary conditions under transverse loads. Their analysis considered uncertainty of material properties and applied loading, but uncertainty of strength parameters and thicknesses were not considered.

There have also been several studies on the reliability analysis of linear and nonlinear laminated composite plates under static and dynamic loads. For example, in 1990, Cederbaum et al. [18] presented a reliability analysis of laminated plates subjected to in-plane random static loads based on Hashin failure criterion for unidirectional fiber composites. Kam et al. [19] presented a reliability analysis of nonlinear laminated composite plates using the finite element method (FEM) and limit state equations. Kam and Chang [20] conducted a reliability analysis of plates subjected to first-ply failure also using limit state equations. Gosling and Polit [21] used the First-Order Reliability Method (FORM) to study shear deformable plates. By using artificial neural networks (ANN) and the Second-Order Reliability Method (SORM), Tawfik et al. [22] analyzed laminated composite plates in free vibration and included the effect of randomness in ply thickness, demonstrating a significant effect on the probability of failure.

The present work aims to present a comprehensive study on the overall stochastic effects of ply orientation, ply thickness, and material properties and strengths on the static first-ply failure of composite laminated plates under uniaxial loads, thus highlighting the importance of considering randomness in such properties. The primary intention of this research is to explore relative relationships between stochastic and deterministic failure predictions, so the simpler classical lamination theory is employed as an alternative to shear deformation theories and the finite element method. As such, the findings of this research are most applicable to thin plates (i.e., aspect ratio greater than 50). Strength ratios are also adopted as a simple metric for determining laminate failure. The study uses three different failure theories and considers various materials in various stacking sequences to investigate if a specific trend is common for all materials or multiple types of stacking sequences. The results focus on not only failure load and probability of failure, as in the case of many previous studies, but also on the failure ply. The paper is organized as follows: Section 2 provides a brief overview of the classical lamination theory, and relevant failure theories. A summary of strength ratios is also provided as it is the output of interest. Section 3 provides a brief overview of the Monte Carlo Simulation technique as well as definitions of relevant statistical metrics used in this work. Section 4 describes the simulation procedure and presents a validation of the developed computational code. Results and discussion are presented in Section 5 and conclusions are summarized in Section 6.

2. Brief overview of the classical lamination theory

Classical lamination theory (CLT) is a direct extension of the Kirchhoff hypothesis for plates [23]. As a well-defined and widely accepted theory, CLT is used for the determination of the stress tensor developed in each ply. CLT begins from the mechanics of a single orthotropic lamina under plane stress and proceeds to define stress and strain variations through the thickness of the laminate. The theory assumes negligible shear strain perpendicular to the midplane of the laminate (i.e., a straight line normal to the midplane remains straight and normal after deformation), as well as negligible strain in the laminate thickness direction. In addition, each lamina is considered perfectly bonded by an infinitesimally thin layer with no slippage between laminae. The laminate essentially acts as a single layer of material. More details can be found in literature (for example [23] and [24]).

2.1. Failure Theories

There are two broad classifications of failure theories:

Limit theories, such as the maximum stress and maximum strain failure theories, which compare local stress/strain components with their corresponding strengths, neglecting the interaction between components.

Interaction theories, such as Tsai-Hill and Tsai-Wu, which consider the interaction between stress components, typically by considering the contribution of each component to the total strain energy within the solid body.

2.1.1. Maximum stress failure criterion

The maximum stress failure theory is related to the maximum normal stress theory by Rankine and the maximum shearing stress theory by Tresca [24]. Global stresses are resolved to local stresses in each lamina and failure is predicted if any of the following inequalities are violated:

$$\begin{aligned} &-\left(\sigma_1^C\right)_{\text{ult}} < \sigma_1 < \left(\sigma_1^T\right)_{\text{ult}}, \quad -\left(\sigma_2^C\right)_{\text{ult}} < \sigma_2 < \left(\sigma_2^T\right)_{\text{ult}}, \\ &-\left(\tau_{12}\right)_{\text{ult}} < \tau_{12} < \left(\tau_{12}\right)_{\text{ult}}, \end{aligned} \tag{1}$$

where σ_1, σ_2 and τ_{12} are the local in-plane stress at any location on a lamina, $(\sigma_i^T)_{\text{ult}}$ and $(\sigma_i^C)_{\text{ult}}$ are the ultimate stress in the i direction ($i = 1, 2$) in tension and compression, respectively, and $(\tau_{12})_{\text{ult}}$ is the ultimate shear strength.

2.1.2. Tsai-Hill failure criterion

The Tsai-Hill criterion is an interaction criterion based on the distortion energy yield criterion for isotropic materials as applied to anisotropic materials and subsequently adapted to unidirectional lamina [24]. Failure is said to occur if the following inequality is violated:

$$\left(\frac{\sigma_1}{X_1}\right)^2 - \left(\frac{\sigma_1\sigma_2}{X_2^2}\right) + \left(\frac{\sigma_2}{Y}\right)^2 + \left(\frac{\tau_{12}}{S}\right)^2 < 1, \tag{2}$$

where

$$X_1 = \begin{cases} \left(\sigma_1^T\right)_{\text{ult}} & \text{if } \sigma_1 > 0 \\ \left(\sigma_1^C\right)_{\text{ult}} & \text{if } \sigma_1 < 0 \end{cases}, \quad X_2 = \begin{cases} \left(\sigma_1^T\right)_{\text{ult}} & \text{if } \sigma_2 > 0 \\ \left(\sigma_1^C\right)_{\text{ult}} & \text{if } \sigma_2 < 0 \end{cases},$$
$$Y = \begin{cases} \left(\sigma_2^T\right)_{\text{ult}} & \text{if } \sigma_2 > 0 \\ \left(\sigma_2^C\right)_{\text{ult}} & \text{if } \sigma_2 < 0 \end{cases}, \quad S = \left(\tau_{12}\right)_{\text{ult}}. \tag{3}$$

2.1.3. Tsai-Wu criterion

The Tsai-Wu criterion is based on the total strain energy theory of Beltrami and applied to lamina in plane stress [24]. Per the Mises-Hencky criterion, failure is assumed to have occurred if the following inequality is violated:

$$H_1\sigma_1 + H_2\sigma_2 + H_6\tau_{12} + H_{11}\sigma_1^2 + H_{22}\sigma_2^2 + H_{66}\tau_{12}^2 + 2H_{12}\sigma_1\sigma_2 < 1, \tag{4}$$

where

$$H_1 = \frac{1}{(\sigma_1^T)_{ult}} - \frac{1}{(\sigma_1^C)_{ult}}, \quad H_{11} = \frac{1}{(\sigma_1^T)_{ult}(\sigma_1^C)_{ult}},$$
$$H_2 = \frac{1}{(\sigma_2^T)_{ult}} - \frac{1}{(\sigma_2^C)_{ult}}, \quad H_{22} = \frac{1}{(\sigma_2^T)_{ult}(\sigma_2^C)_{ult}}, \tag{5}$$
$$H_6 = 0, \quad H_{66} = \frac{1}{(\tau_{12})_{ult}^2}, \quad H_{12} = -\frac{1}{2}\sqrt{\frac{1}{(\sigma_1^T)_{ult}(\sigma_1^C)_{ult}(\sigma_2^T)_{ult}(\sigma_2^C)_{ult}}}.$$

The H_{12} component is the only component that cannot be determined from the strength parameters of the unidirectional lamina and must be found experimentally [24]. The Mises-Hencky criterion for H_{12} provided in Eq. (5) is an empirical suggestion and is used in this research.

2.1.4. Strength ratios

The failure theories described in Sections 2.1.1–2.1.3 allow one to detect failure as a Boolean (i.e., "true" or "false") value, but they provide very little information on how much the applied load can be increased if the laminate is safe or decreased if the laminate fails [24]. The strength ratio is a particularly useful concept as it is applicable to any failure theory and is accordingly used to compare all failure theories considered in this research. The strength ratio is a simple metric defined as

$$\mathrm{SR} = \frac{F_{\max}}{F_{\text{applied}}}, \tag{6}$$

where F_{applied} is the applied load and $F_{\max}$ is the maximum load which can be applied before the selected failure criterion is violated.

In order to use the failure theories to calculate the strength ratios and the first-ply failure loads, we assume that the forces and moment per unit length (N_x, N_y, N_{xy}, M_x, M_y, M_{yx}) applied on the composite plate are multiplied by the strength ratio (SR).

$$\begin{Bmatrix} \boldsymbol{\varepsilon}^{\mathbf{0}} \\ \boldsymbol{\kappa} \end{Bmatrix} = \begin{bmatrix} \mathbf{A}^* & \mathbf{B}^* \\ \mathbf{C}^* & \mathbf{D}^* \end{bmatrix} \begin{Bmatrix} \mathbf{N} \\ \mathbf{M} \end{Bmatrix} \mathrm{SR}; \quad \text{where} \quad \begin{bmatrix} \mathbf{A}^* & \mathbf{B}^* \\ \mathbf{C}^* & \mathbf{D}^* \end{bmatrix} = \begin{bmatrix} \mathbf{A} & \mathbf{B} \\ \mathbf{B} & \mathbf{D} \end{bmatrix}^{-1}. \tag{7}$$

$\boldsymbol{\varepsilon}^{\mathbf{0}}$ and $\boldsymbol{\kappa}\boldsymbol{\kappa}$ are the midplane strains and curvatures, **A**, **B** and **D** matrices are the laminate's extensional, coupling and bending stiffness matrices, respectively [24], $\mathbf{N} = [\ N_x \quad N_y \quad N_{xy}\ ]^T$, and $\mathbf{M} = [\ M_x \quad M_y \quad M_{xy}\ ]^T$.

The global strain at any height z in lamina k of the laminate can be obtained from the midplane strains and curvatures as:

$$(\boldsymbol{\varepsilon}_G)_k = \boldsymbol{\varepsilon}^{\mathbf{0}} + z\boldsymbol{\kappa} = (\bar{\boldsymbol{\varepsilon}}^{\mathbf{0}} + z\bar{\boldsymbol{\kappa}})\mathrm{SR}. \tag{8}$$

The local stresses at any height z in lamina k can also be obtained as:

$$(\boldsymbol{\sigma}_L)_k = \mathbf{S}_k^{-1}(\boldsymbol{\varepsilon}_L)_k = \mathbf{S}_k^{-1}\left[\mathbf{T}_k^{-1}(\boldsymbol{\varepsilon}_G)_k\right] = \mathbf{S}_k^{-1}\mathbf{T}_k^{-1}(\bar{\boldsymbol{\varepsilon}}^{\mathbf{0}} + z\bar{\boldsymbol{\kappa}})\mathrm{SR}, \tag{9}$$

where $\mathbf{S}_k = \mathbf{S}_k(E_{11}, E_{22}, G_{12}, \nu_{12})$ and $\mathbf{T}_k = \mathbf{T}_k(\theta_k)$ are the reduced compliance matrix and transformation matrix of ply k, respectively [24], and E_{11}, E_{22}, G_{12}, ν_{12} and θ_k are ply k's two Young's moduli, shear modulus, Poisson's ratio and fiber-orientation angle, respectively. So the in-plane components of the local strain tensor at any height z in lamina k can be written as $(\sigma_1)_k = m_k\mathrm{SR}$, $(\sigma_2)_k = n_k\mathrm{SR}$ and $(\tau_{12})_k = p_k\mathrm{SR}$. Using these expressions of local stresses, we can obtain the strength ratio that can be multiplied by the applied loads to cause first-ply failure. For the maximum stress failure theory, three values of strength ratios, corresponding to the three sub-criteria, can be obtained for each ply k. The failure load for this ply would be the minimum of these three values, and is expressed as follows:

$$\mathrm{SR}_{k(Max.Stress)} = \min\left[\frac{(\sigma_1^{T/C})_{ult}}{|m|} \quad \frac{(\sigma_2^{T/C})_{ult}}{|n|} \quad \frac{(\tau_{12})_{ult}}{|p|}\right]_k, \tag{10}$$

where the tensile and compressive ultimate strengths are selected according to the local stress condition (i.e., $(\sigma_i^T)_{ult}$ is used if m_k is positive). For Tsai-Hill and Tsai-Wu failure theories, respectively, the maximum applied load in lamina k can be expressed as

$$\mathrm{SR}_{k(Tsai-Hill)} = 1/\sqrt{\left(\frac{m}{X_1}\right)_k^2 - \left(\frac{mn}{X_2^2}\right)_k + \left(\frac{n}{Y}\right)_k^2 + \left(\frac{p}{S}\right)_k^2}, \tag{11}$$

$$\mathrm{SR}_{k(Tsai-Wu)} = \frac{-B_k + \sqrt{B_k^2 + 4A_k}}{2A_k}; \qquad B_k = H_1 m_k + H_2 n_k + H_6 p_k, \tag{12}$$
$$A_k = H_{11}m_k^2 + H_{22}n_k^2 + H_{66}p_k^2 + 2H_{12}m_k n_k.$$

The strength ratio for the whole laminate is then defined as the minimum value of SR_k among all plies.

$$\mathrm{SR} = \min_k\left(\mathrm{SR}_k\right). \tag{13}$$

3. Brief overview of technique and statistical metrics

3.1. Monte Carlo simulation

Monte Carlo simulation (MCS) is a common and simple computational approach to stochastic problems. It is particularly useful in physical problems with many degrees of freedom and as such is used to generate the data used in this research. MCS involves repeated sampling of random variables to simulate an arbitrarily large number of experiments and obtain numerical results. For each trial in this study the material properties, material strengths ply orientations, and ply thickness form a vector, **X**, of basic random variables given by

$$\mathbf{X} = \Big[\ \underbrace{\begin{pmatrix} E_{11} & E_{22} & G_{12} & \upsilon_{12} & \theta & t \end{pmatrix}_1 \cdots \begin{pmatrix} E_{11} & E_{22} & G_{12} & \upsilon_{12} & \theta & t \end{pmatrix}_n}_{n} \ \underbrace{(\sigma_1^T)_{ult} \quad (\sigma_1^C)_{ult} \quad (\sigma_2^T)_{ult} \quad (\sigma_2^C)_{ult} \quad (\tau_{12})_{ult}}_{5}\ \Big]. \tag{14}$$

All material properties and geometric parameters are allowed to vary at the ply level, but for simplicity, ultimate ply strengths are assumed to be equal for all plies in a given laminate. The vector of stochastic input variables **X** in (14) highlights the increasing complexity and uncertainty of the laminate strength ratio as a random variable. For the type of problem considered in this study, a laminate of only two plies possesses 17 stochastic degrees of freedom. As the number of layers increases, the number of random variables increases linearly as $6n$. The total number of random variables in a laminate of n plies made of the same material is $6n+5$.

3.2. Probability of failure and correction factor

The probability of failure is defined in this study as the proportion of laminates in a simulation of N trials whose resulting strength ratio is less than the predicted deterministic value, SR_D, and can be calculated as

$$P_f = \frac{1}{N}\sum_{i=1}^{N} I\left(\mathrm{SR}_i < \mathrm{SR}_D\right), \tag{15}$$

where $I(\mathrm{SR}_i < \mathrm{SR}_D)$ is the indicator function of laminate failure, defined as

$$I\left(\mathrm{SR}_i \le \mathrm{SR}_D\right) = \begin{cases} 1 & \text{if} \mathrm{SR}_i \le \mathrm{SR}_D \\ 0 & \text{if} \mathrm{SR}_i > \mathrm{SR}_D \end{cases}, \tag{16}$$

and the strength ratio, SR_i, is a realization of the random variable, SR, defined as a function of the random variable **X** in trial i, i.e. $\mathrm{SR}_i = \mathrm{SR}(\mathbf{X}_i)$.

Defining failure probability in this way results in an issue similar to the Boolean failure criteria in Section 2, namely that there is little information provided on the degree of the laminate failure. To address this, the correction factor (CF) is defined as

$$\mathrm{CF} = \frac{\mathrm{SR}_D}{\mathrm{SR}_{Failed}}, \tag{17}$$

where SR_{Failed} is the strength ratio of the failed laminate (i.e. $SR_{Failed} = SR_i$ when $SR_i \geq SR_D$). Hence, CF is defined only when the laminate fails. CF can be interpreted as the factor by which the strength ratio of a laminate must be multiplied by to reach the predicted deterministic value. It also provides a means to compare the relative magnitudes of failure between simulation trials.

3.3. The empirical distribution function and sample quantiles

The cumulative distribution function (CDF) of a random variable, Y, is used to describe the distribution of that random variable. It is defined as

$$F_Y(y) = \mathrm{P}(Y \leq y), \quad y \in R. \tag{18}$$

The CDF is a useful way to visualize the distribution of a random variable, Y, as it can be interpreted as the probability of observing a value less than or equal to some realization of the random variable (y). More importantly, the CDF effectively contains all information about the random variable and completely determines the shape of its distribution. The CDF can be approximated by

$$\hat{F}_Y(y) = \frac{1}{N}\sum_{i=1}^{N} I\left(Y_i < y\right), \tag{19}$$

which is also known as the empirical distribution function (EDF) [25]. The EDF of the strength ratio can therefore be defined as

$$\hat{F}_{\mathrm{SR}}(x) = \frac{1}{N}\sum_{i=1}^{N} I\left(\mathrm{SR}_i < x\right), \quad \min\{\mathrm{SR}\} \leq x < \max\{\mathrm{SR}\}, \tag{20}$$

where min{SR} and max{SR} are the lowest and highest realizations of the strength ratio of all trials in a given simulation. From Eq. (20), the definition of the g^{th} sample quantile follows as

$$\hat{F}^{-1}_{\mathrm{SR}}(g) = \inf\left\{x : \hat{F}_{\mathrm{SR}}(x) \geq g\right\}, \tag{21}$$

which represents the value of the strength ratio or correction factor beneath which a proportion g of laminates falls below. For instance, if $g = 0.5$ (50%), Eq. (21) would return the sample median strength ratio or correction factor. inf{ } is the infimum function.

4. Simulation set-up and code validation

4.1. Procedure

A MATLAB code was written to compute the strength ratios of various laminates using CLT and each of the failure theories described in Sections 2.1.1–2.1.3. Strength ratio data were generated using MCS for five different simulations which consider various combinations of material and laminate parameters to explore the interaction effects of randomness in each parameter. Coefficients of variation were held constant for each simulation with values in the interval [0.01, 0.20] and increments of 0.01. Each simulation was repeated for 5,000 trials, resulting in a total of 100,000 trials for each combination of laminate and material. The random seed was reset in between simulations to isolate the interaction effects. The MATLAB code schematic is shown in Fig. 1. A summary of simulations performed is provided in Table 1.

Materials examined and their corresponding mean values are summarized in Table 2. These materials were used in [24] as well. Elastic and shear moduli are given in units of GPa and strengths are given in MPa. Ply thickness is given in meters. The standard deviations of all material properties are defined in the MATLAB code as functions of their mean values and CV. An exception is made for the ply orientation, whose standard deviation is assumed to have a maximum of 1.8° at the upper bound of simulated CV values and varies linearly with CV (e.g., the deviation is 0.9° for CV=0.10) as in [22].

Experimental data from Maekawa [7] regarding material properties of unidirectional carbon fiber-reinforced laminates shows that the distribution of basic material parameters can be closely approximated by a Gaussian or normal distribution. Using the Kolmogorov-Smirnov test, Lekou and Philippidis [6] showed that the assumption of normally distributed mechanical properties for unidirectional glass/polyester cannot be rejected at the 5% significance level. Thus, the assumption of normally distributed material properties, strengths, ply thicknesses, and ply orientations for the present analysis is valid.

4.2. Code validation

The CLT analysis coded in MATLAB considers a square plate of unit length subjected to a pure tensile load of in the global x-direction (i.e., $N_x = 1\ N/m,\ N_y = N_{xy} = M_x = M_y = M_{xy} = 0$). Given this loading condition, the strength ratios reported in this research are equivalent to the first-ply failure loads. Table 3 lists the various laminates considered in this research.

First-ply failure load results were validated against literature [24] for a [0 90 0] graphite/epoxy laminate subjected to a unidirectional tensile load in the x-direction with ply thicknesses of 5 mm. Tsai-Wu strength ratios for each ply at various elevations of the ply are shown in Table 4, which demonstrates complete agreement with the developed MATLAB code. Results for other failure theories show similar agreement and are not shown.

First-ply failure load results were also validated against a converged finite element model created on a commercial finite element analysis software (SolidWorks Simulation 2019 Package). Laminates are modeled as square planes with unit area and the bottom left corner is fixed at the origin of the global coordinate system as shown in orange in Fig. 2. Translation at the left and bottom edges is restricted in the perpendicular direction and rotation is restricted about the z-axis and in the edge direction. The top and right edges are free and the default mesh size is used.

Results of the finite element analysis are summarized in Table 5, which shows a good agreement between the results of the MATLAB code and the commercial software both in terms of the calculated first-ply failure load and the predicted failure ply. In particular, the results of the cross-ply laminate are identical. Deviation occurs with non-cross-ply laminates due to the difference in analysis technique, namely the propagation of element-wise coupling effects in using the finite element method. Values for these laminates reported in Table 5 are median values on the midplane and were manually retrieved from the raw SolidWorks simulation data. It is also noted that for laminates 2 and 5, the limit and interaction failure theories result in different predicted failure ply which are all correctly determined by the MATLAB code.

5. Results and discussion

5.1. Strength ratio coefficient of variation

Figs. 3–7 show an increasing strength ratio coefficient of variation (CV(SR)) with input coefficient of variation (CV(**X**)) for all laminates considered in this study. The figures again demonstrate the validity of the MATLAB code as similar conclusions were drawn for both cross-ply and non-cross-ply laminates in [14] and [22]. It is apparent that the linear increase in natural frequency and displacement coefficients of variation found in [14] and [22] is also mirrored for the strength ratio.

Table 6 provides a summary of linear fit slopes for all combinations of stacking sequence, material, and simulation. Across all laminates and materials, the average slope is 1.2402 when considering all material properties and parameters as random. This indicates that across all simulations, each unit change in CV(**X**) results in a 24% greater response in the CV(SR) which is significantly disproportionate. All linear fits are correlated with an average minimum correlation coefficient of 0.997 across

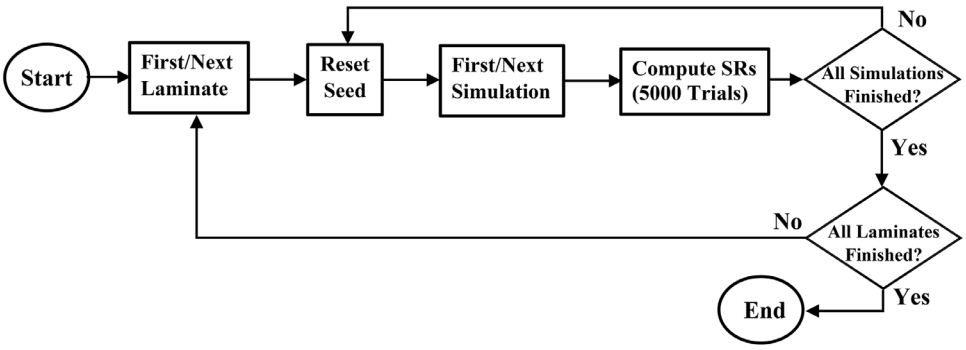

Fig. 1. MATLAB code flow chart.

Table 1
List of simulations performed.

Simulation	Random parameters
1	Material properties only
2	Material properties and ply orientation
3	Material properties and ply thickness
4	Material properties, ply orientation, and ply thickness
5	Material properties, ply orientation, ply thickness and material strengths

Table 2
Mean material properties and parameters.

Material	E_{11}	E_{22}	G_{12}	υ_{12}	$(\sigma_1^T)_{ult}$	$(\sigma_1^C)_{ult}$	$(\sigma_2^T)_{ult}$	$(\sigma_2^C)_{ult}$	$(\tau_{12})_{ult}$	$\Delta\theta$	t
Graphite/epoxy	181	10.30	7.17	0.28	1500	1500	40	246	68	0.0^0	0.005
Glass/epoxy	38.6	8.27	4.14	0.26	1062	610	31	118	72	0.0^0	0.005
Boron/epoxy	204	18.50	5.59	0.23	1260	2500	61	202	67	0.0^0	0.005

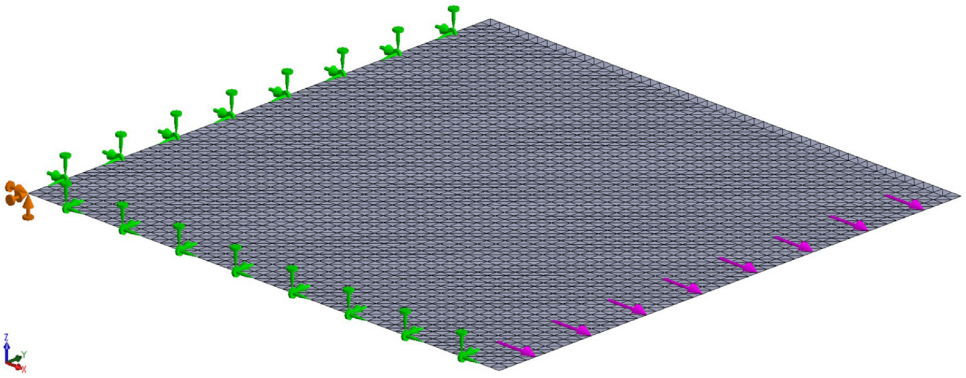

Fig. 2. Solidworks model with boundary conditions, load, and mesh.

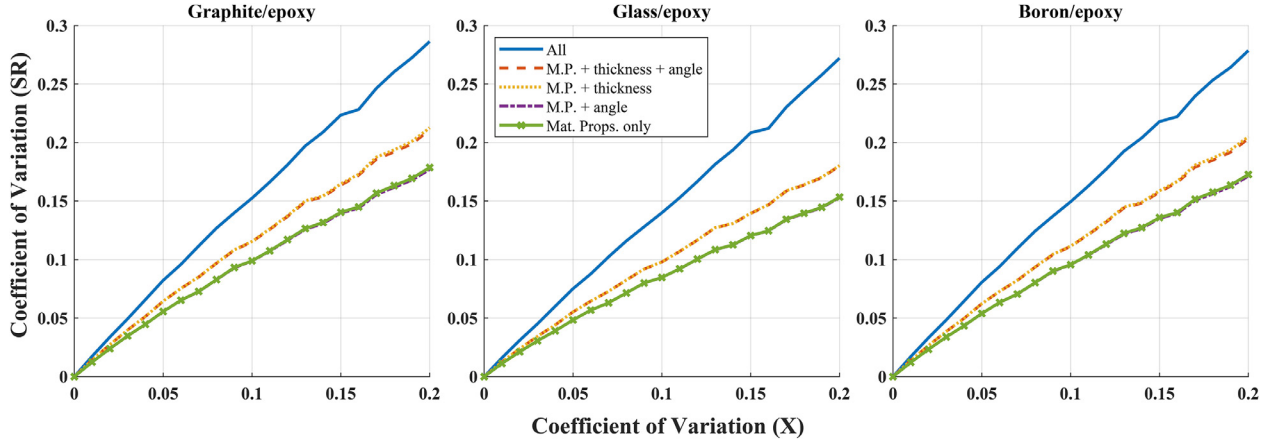

Fig. 3. Coefficients of variation: Input variables vs. Tsai-Wu strength ratios, Laminate 1 (M.P. means Material Properties).

Table 3
List of studied laminates.

Laminate	Type of laminate	Stacking Sequence
1	Cross-ply, unsymmetric	$[0\ 90\ 90\ 0\ 90\ 90\ 0\ 0]_T$
2	Balanced	$[30\ 40\ -30\ 30\ -30\ -40]_T$
3	Angle-ply, balanced	$[-40\ 40\ -40\ 40]_T$
4	Angle-ply, symmetric	$[-40\ 40\ -40\ 40\ -40]_T$
5	Antisymmetric, balanced	$[45\ 60\ -60\ -45]_T$

Table 4
Comparison of Tsai-Wu strength ratios for [0 90 0] graphite/epoxy laminate.

Ply Number	Position	Kaw [24]	MATLAB	Δ%
1	Top	1.339E+07	1.339E+07	0.00
	Middle	1.339E+07	1.339E+07	0.00
	Bottom	1.339E+07	1.339E+07	0.00
2	Top	7.277E+06	7.277E+06	0.00
	Middle	7.277E+06	7.277E+06	0.00
	Bottom	7.277E+06	7.277E+06	0.00
3	Top	1.339E+07	1.339E+07	0.00
	Middle	1.339E+07	1.339E+07	0.00
	Bottom	1.339E+07	1.339E+07	0.00

Table 6
Trendline slopes: $CV(SR_{Tsai\text{-}Wu})$ vs. CV(**X**).

	Graphite/epoxy				
Laminate	Sim 1	Sim 2	Sim 3	Sim 4	Sim 5
1	0.8704	0.8619	1.0405	1.0304	1.4125
2	0.6588	0.7074	0.8715	0.9079	1.3037
3	0.387	0.5008	0.6468	0.7244	1.2326
4	0.3977	0.4855	0.6005	0.6627	1.2148
5	0.3053	0.3399	0.6021	0.6216	1.0536
	Glass/epoxy				
Laminate	Sim 1	Sim 2	Sim 3	Sim 4	Sim 5
1	0.74146	0.73981	0.87852	0.87668	1.333
2	0.7926	0.8132	0.9703	0.9847	1.2812
3	0.6386	0.711	0.888	0.9382	1.2718
4	0.4936	0.5819	0.6986	0.7596	1.1748
5	0.4297	0.436	0.6663	0.6707	1.1551
	Boron/epoxy				
Laminate	Sim 1	Sim 2	Sim 3	Sim 4	Sim 5
1	0.84001	0.83257	1.0019	0.99231	1.3718
2	0.612	0.6914	0.8389	0.8944	1.244
3	0.4023	0.5396	0.6517	0.7486	1.2507
4	0.3991	0.5118	0.603	0.6837	1.2252
5	0.3573	0.3567	0.6195	0.6203	1.0786

all laminates and simulations. Only values for Tsai-Wu failure theory are shown as other failure theories generate nearly identical results.

Table 6 also indicates that the slope magnitudes are heavily dependent on stacking sequence. For simulation 5, the CV(SR) of laminate 5 exhibits an average slope of 1.0958 across all materials while the average for laminate 1 is 1.3725. In other words, the response of CV(SR) is only 9.58% higher for each unit change of CV(**X**) for laminate 5 compared 37.25% for laminate 1 – nearly four times greater an effect. This difference in behavior between laminates 1 and 5 is explored in more depth in Section 5.5, where it is shown that increasing CV(**X**) results in different first-ply failures. For laminate 1, this behavioral change potentially result in higher strength ratios, which is not typically true for laminate 5. Because CV(SR) describes the dispersion of strength ratios relative to the mean value, CV(SR) is greater for laminate 1.

In their paper, Tawfik et al. [22] found that ply angle randomness was negligible for a [0 90] cross-ply laminate but significant for a [0 45 -45 90] laminate, which shows a dependence on stacking sequence when considering ply angle individually as a random variable. Figs. 4–6 confirm this for non-cross-ply laminates. Laminate 5 (Fig. 7) does not show this significance, suggesting that, similar to cross-ply laminates, the effect of randomness in the ply angle is not significant for anti-symmetric laminates.

Independent of stacking sequence, material, and failure theory, the greatest effect on CV(SR) is due to thickness as found in [15] and [22], and material strength, whose importance was highlighted but not tested in [15]. The importance of thickness was also reported by Gohari et al. [26], who found that slight changes in shell lay-up thickness caused considerable fluctuations in failure strength. Subsequent studies in Sections 5.2 through 5.5 are performed for simulation 5 (all parameters random) unless otherwise noted.

5.2. Probability of failure

Fig. 8 shows the convergence of the Monte Carlo simulation results for laminate 3, which converges to less than 1% relative error for all nine combinations of material and failure theory, averaged over all values of CV. As convergence studies for all other laminates return similar results, the figure shown is specifically for laminate 3 since glass/epoxy under the Maximum Stress criterion demonstrated the most distinct behavior relative to any other laminate. Regardless, mean error for all laminates converges to below 1.5% for 5000 trials, demonstrating that 5000-trials is a suitable stopping point.

Figs. 9–13 show the probability of failure for the five considered laminates in three materials using all considered failure theories. It can

Table 5
Comparison of SolidWorks model and MATLAB code solutions.

		First-ply failure load (N/m)			Failed Ply	
Laminate	Theory	SolidWorks	MATLAB	Δ%	SolidWorks	MATLAB
1	Max. Stress	1.236E+07	1.236E+07	0.00	2	2
	Tsai-Hill	1.236E+07	1.236E+07	0.00	2	2
	Tsai-Wu	1.235E+07	1.235E+07	0.00	2	2
2	Max. Stress	6.987E+06	7.140E+06	-2.19	1	1
	Tsai-Hill	6.688E+06	6.746E+06	-0.87	6	6
	Tsai-Wu	6.217E+06	6.075E+06	2.28	6	6
3	Max. Stress	3.149E+06	3.192E+06	-1.37	4	4
	Tsai-Hill	3.140E+06	3.184E+06	-1.39	4	4
	Tsai-Wu	3.096E+06	3.113E+06	-0.54	4	4
4	Max. Stress	4.071E+06	4.076E+06	-0.13	3	3
	Tsai-Hill	4.051E+06	4.057E+06	-0.15	3	3
	Tsai-Wu	4.190E+06	4.187E+06	0.07	3	3
5	Max. Stress	1.427E+06	1.368E+06	4.17	2	2
	Tsai-Hill	1.263E+06	1.220E+06	3.40	1	1
	Tsai-Wu	1.184E+06	1.133E+06	4.28	1	1

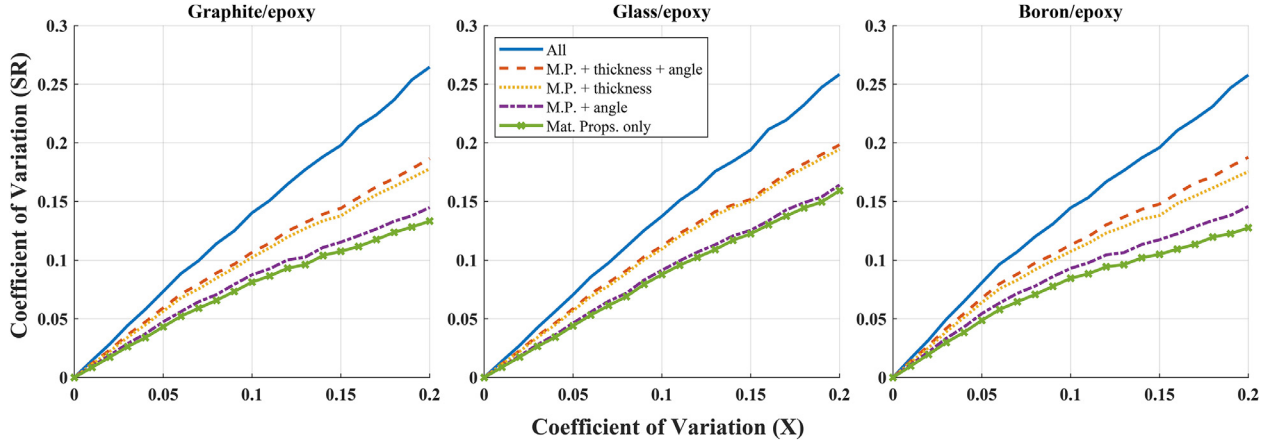

Fig. 4. Coefficients of variation: Input variables vs. Tsai-Wu strength ratios, Laminate 2.

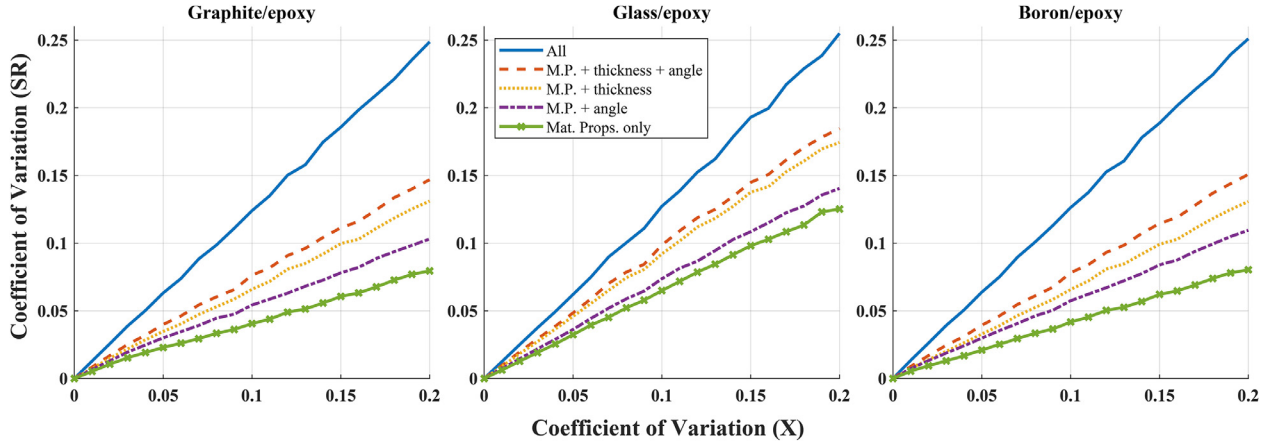

Fig. 5. Coefficients of variation: Input variables vs. Tsai-Wu strength ratios, Laminate 3.

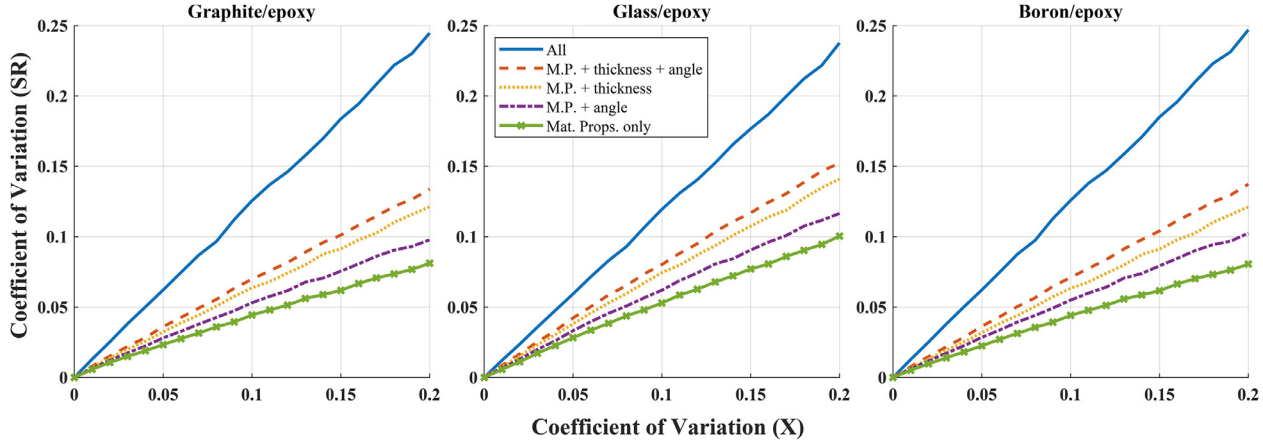

Fig. 6. Coefficients of variation: Input variables vs. Tsai-Wu strength ratios, Laminate 4.

be concluded that failure probability is generally non-linear and highly dependent on the combination of stacking sequence, failure theory, and material. Failure is much less predictable for non-cross-ply laminates, likely because there is a greater influence of randomness when there are additional coupling effects due to the different stacking sequences.

The dependence of failure probability on the particular combination of design factors is highlighted in Figs. 10–13, which indicate significant interaction between failure theory, material, and stacking sequence. In particular, Fig. 11 shows considerably different behavior for glass/epoxy under the maximum stress failure criterion. This is a contrary to the deterministic cases studied by Rattanawangcharoen [2] and Reddy and Pandey [27], who concluded that all failure criteria are equivalent in predicting failure of laminates subjected to in-plane loads. While there are several scenarios in which failure theories are in close agreement, there are more cases where they exhibit very different behavior; as reported by Lopez et al. [28], no criterion is always the most or least conservative, which highlights the caution that must be exercised in selecting a failure criterion.

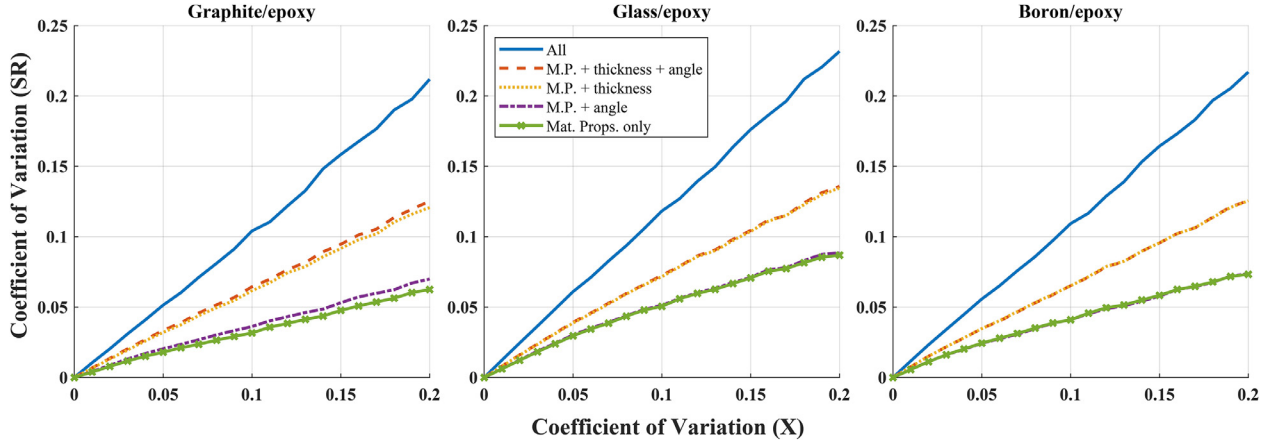

Fig. 7. Coefficients of variation: Input variables vs. Tsai-Wu strength ratios, Laminate 5.

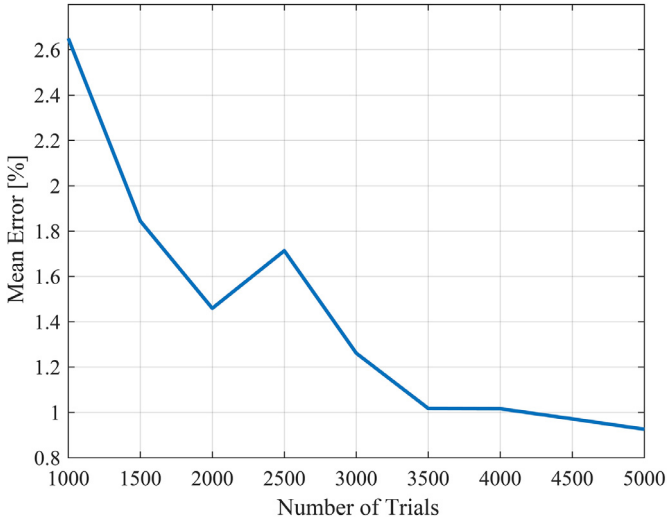

Fig. 8. Mean relative error for Monte Carlo simulations at 500 trial increments, Laminate 3.

5.3. Correction factor

Fig. 14 shows a strong, positive correlation between the mean correction factor and CV(**X**). The mean is chosen because it is less robust to outliers than the median and is therefore a more conservative measure. The correction factor is generally less dependent on the combination of stacking sequence, failure theory, and material than the probability of failure.

Table 7 provides a comprehensive summary of the linear fit slopes for all laminate, material, and failure theory combinations, which are all correlated with an average minimum correlation factor of 0.993.

For almost any laminate and material combination there is a general agreement in the mean correction factor between all failure theories, which is why most figures are omitted. Laminate 3 is an exception, however, showing a relatively more extreme response of the mean CF for glass/epoxy under the maximum stress failure theory. This is undoubtedly connected to the distinct failure probability shown in Fig. 11 (middle), but also indicates that, for this combination of failure theory, material, and stacking sequence, laminates which do not meet the deterministic value simultaneously miss it by relatively larger margins.

From Table 7, the slope for Laminate 3 in this case is seen to be 2.7079, which means that for every 1% increase in CV(**X**) there is a corresponding additive increase of 2.7% to the mean correction factor. As with the strength ratio, CV(**X**) for laminate 5 seems to exhibit a lesser magnitude of effect on the mean correction factor. Laminate 1 shows an average slope of 2.0125 across all failure theories for graphite/epoxy, while laminate 5 is only 1.6302.

Fig. 15 shows the EDF of the Tsai-Wu and maximum stress factors of safety for laminates 1 and 3, respectively. The EDFs for other laminate/theory combinations are nearly identical and are thus omitted. Table 8 summarizes sample quantiles for mean correction factor for

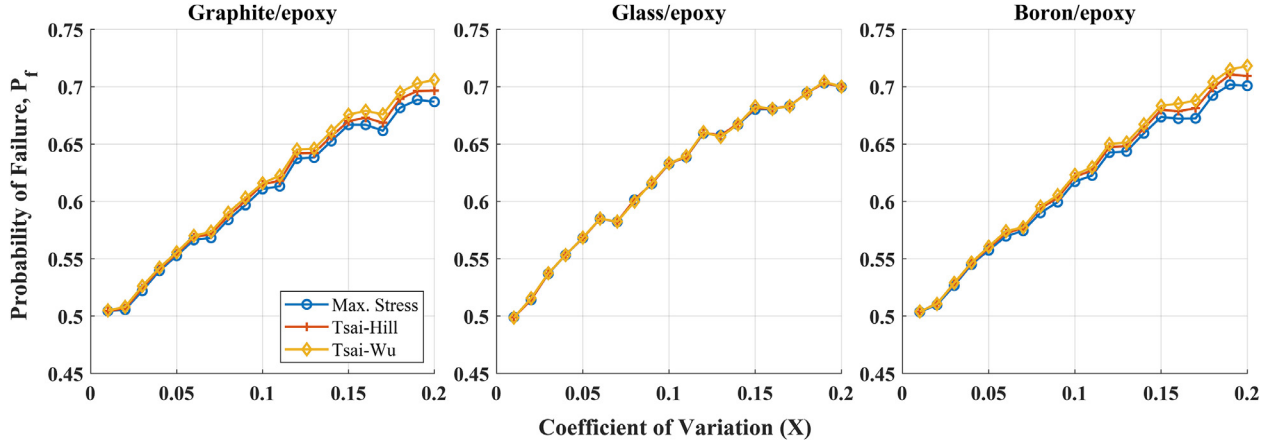

Fig. 9. Probability of Failure: Theory comparison, Laminate 1.

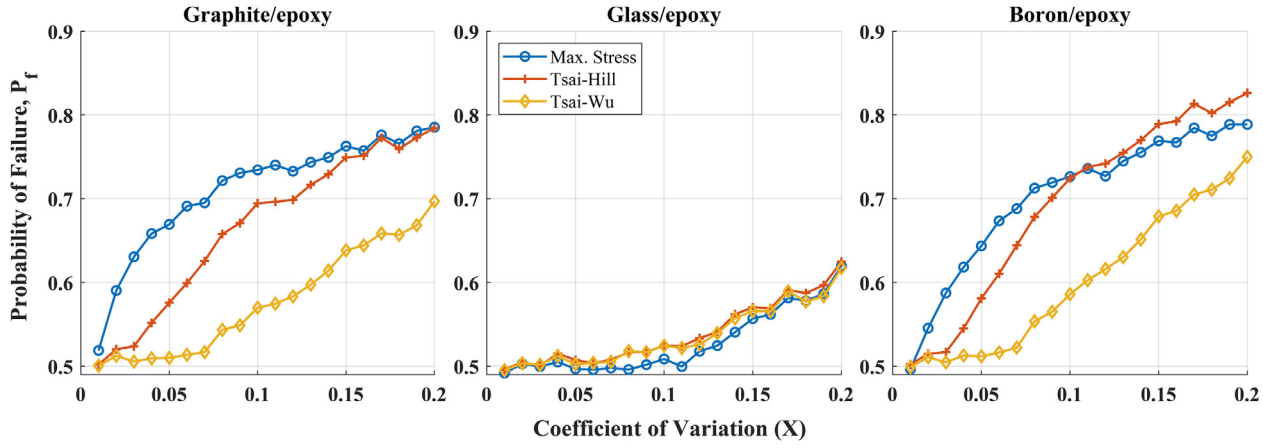

Fig. 10. Probability of Failure: Theory comparison, Laminate 2.

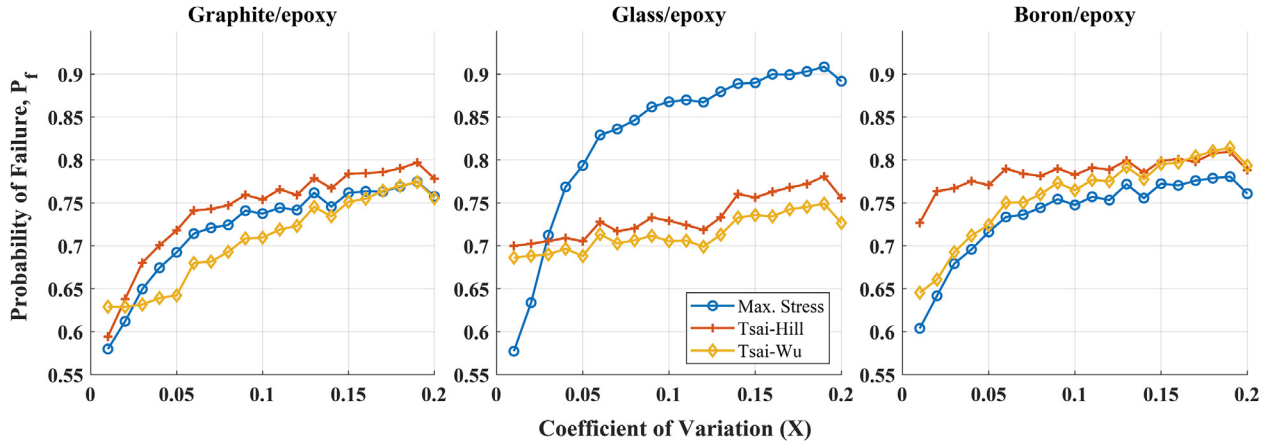

Fig. 11. Probability of Failure: Theory comparison, Laminate 3.

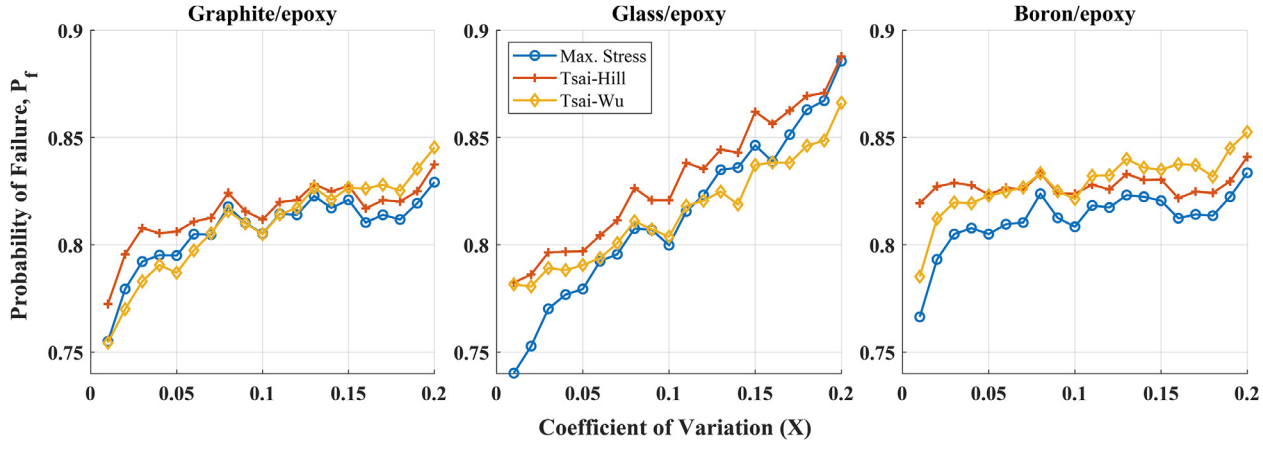

Fig. 12. Probability of Failure: Theory comparison, Laminate 4.

Table 7
Mean $CF_{Tsai\text{-}Wu}$ vs. CV(X): Trendline slopes.

	Graphite/epoxy			Glass/epoxy			Boron/epoxy		
Laminate	Max. Stress	Tsai-Hill	Tsai-Wu	Max. Stress	Tsai-Hill	Tsai-Wu	Max. Stress	Tsai-Hill	Tsai-Wu
1	2.0088	2.0141	2.0147	1.8566	1.8569	1.8495	1.9713	1.9753	1.9783
2	1.8556	1.8423	1.6893	1.8058	1.5102	1.4700	1.9619	1.9229	1.8418
3	1.8308	1.8572	1.8257	2.7079	1.8100	1.7637	1.8622	1.8803	1.9698
4	1.8979	1.8925	2.0056	2.0994	1.9897	1.9816	1.9128	1.8893	2.0468
5	1.8439	1.5823	1.4643	1.6817	1.6251	1.5946	1.6358	1.5372	1.5451

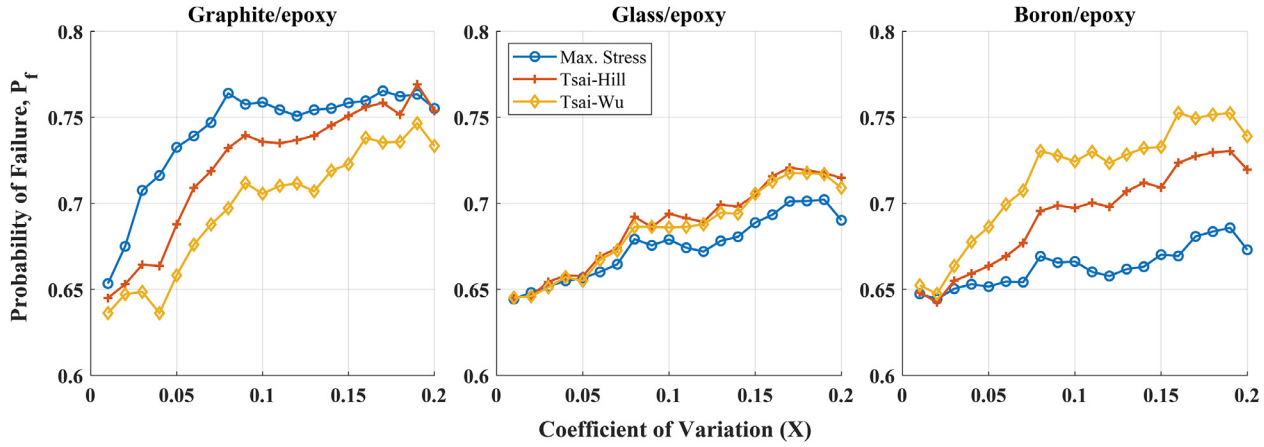

Fig. 13. Probability of Failure: Theory comparison, Laminate 5.

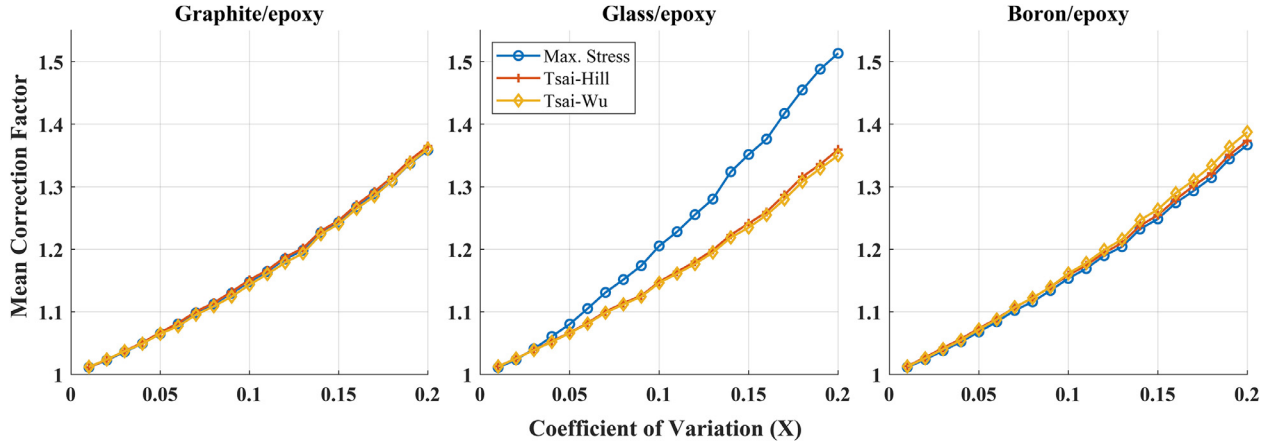

Fig. 14. Correction factor: Theory comparison, Laminate 3.

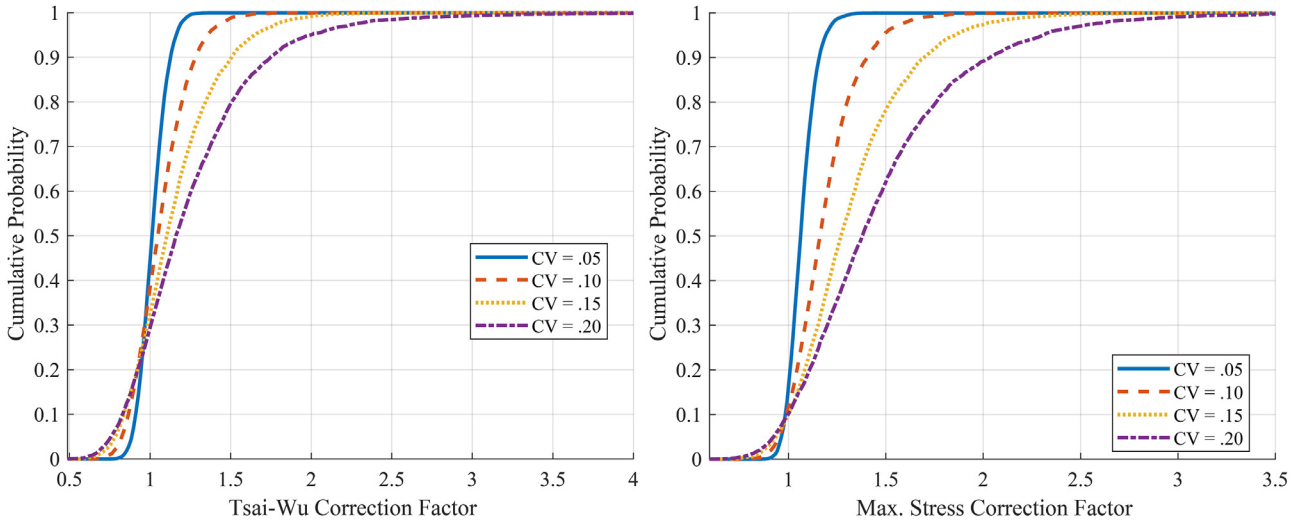

Fig. 15. Correction factor EDF: Graphite/Epoxy, Laminate 1 (left); Glass/Epoxy, Laminate 3 (right).

only one combination of material and failure theory. These EDFs clearly demonstrate that the sample quantiles of the factors of safety increase significantly with CV(**X**). For laminate 1 of graphite/epoxy, 90% of simulated laminates have a correction factor less than or equal to 1.1269 when CV(**X**) is 0.05, but 1.7474 when CV(**X**) is 0.20. In other words, with CV=0.05, 90% of laminates must be designed up to 13% stronger to ensure the expected deterministic strength ratio is attained, compared to 75% when considering CV=0.20 – a difference nearly 6 times greater. For glass/epoxy laminate 3, the disparity is even more pronounced as shown in Fig. 15 (right). These results agree with the findings of Khasaba et al. [29], who concluded that there is a large penalty paid to gain high reliability.

Table 8
$CF_{Tsai\text{-}Wu}$: Sample quantiles (graphite/epoxy).

	90th			95th			99th		
Laminate	CV = 0.05	CV = 0.10	CV = 0.20	CV = 0.05	CV = 0.10	CV = 0.20	CV = 0.05	CV = 0.10	CV = 0.20
1	1.1269	1.2829	1.7474	1.1622	1.3573	1.9955	1.2282	1.5124	2.7212
2	1.0976	1.231	1.6358	1.13	1.2983	1.8319	1.1923	1.4211	2.2885
3	1.1139	1.2592	1.6679	1.1408	1.3219	1.8589	1.1915	1.4497	2.3959
4	1.1399	1.316	1.7773	1.169	1.3901	1.9983	1.2224	1.5437	2.4876
5	1.0912	1.2098	1.5283	1.1148	1.2596	1.6818	1.1586	1.3734	2.0943

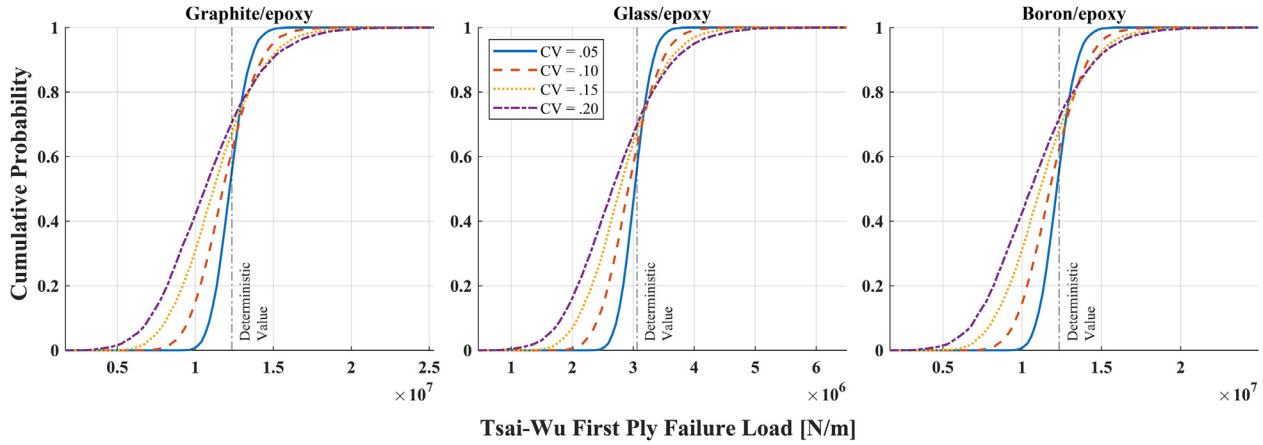

Fig. 16. Tsai-Wu first-ply failure load: EDF, Laminate 1.

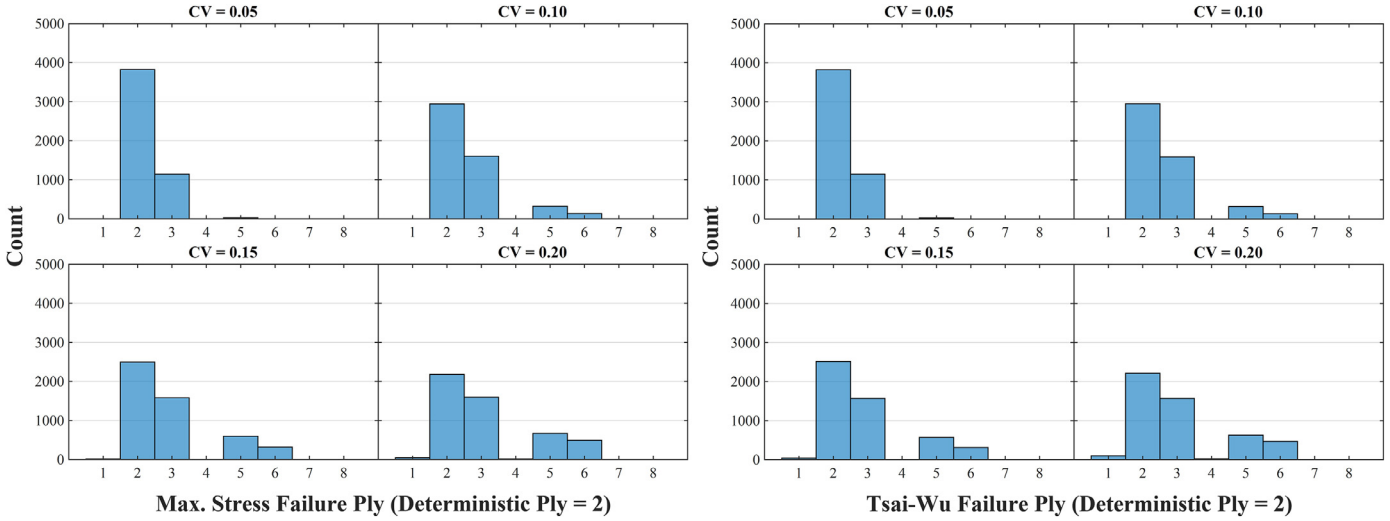

Fig. 17. Failure ply distributions, Graphite/epoxy, Laminate 1.

5.4. *Strength ratio empirical distribution functions*

Fig. 16 shows the EDFs of the Tsai-Wu strength ratios for laminate 1 with varying degrees of CV(**X**). In all cases, there is an increasing variation in the strength ratio as CV(**X**) increases, as indicated by the widening shapes of the EDFs, similar to the mean factors of safety. The EDFs of other simulations are nearly identical and are thus omitted.

5.5. *Failure Ply*

Figs. 17–20 show the distribution of failure plies for various magnitudes of CV(**X**). The distributions for most combinations of material and failure theories are nearly identical and are thus omitted. Independent of the combination of stacking sequence, material, and failure theory, the variation in the failure ply increases with CV(**X**).

Interaction theories appear to be particularly sensitive to the increasing variation since they consider all components of stress. Laminates 4 and 5 which are symmetric and anti-symmetric laminates, respectively, also appear to have symmetric failure ply distributions. In addition, the deterministic plies predicted by CLT fail with the highest empirical probability, but that probability is not as pronounced as for laminate 1. For instance, in the case of laminate 5, the ply opposite to the deterministic failed ply about the midplane fails with essentially equal probability, even for the smallest displayed value of CV. This is true for both maximum stress and Tsai-Wu failure theories.

Although graphite/epoxy and boron/epoxy exhibit similar failure ply distributions in almost all scenarios, glass/epoxy tends to have more distinct behavior as demonstrated by comparing Figs. 19 and 20. For example, for graphite/epoxy at CV=0.05, the failure ply distribution for Tsai-Wu predicts most failures to happen in plies 1 and 4, with fewer

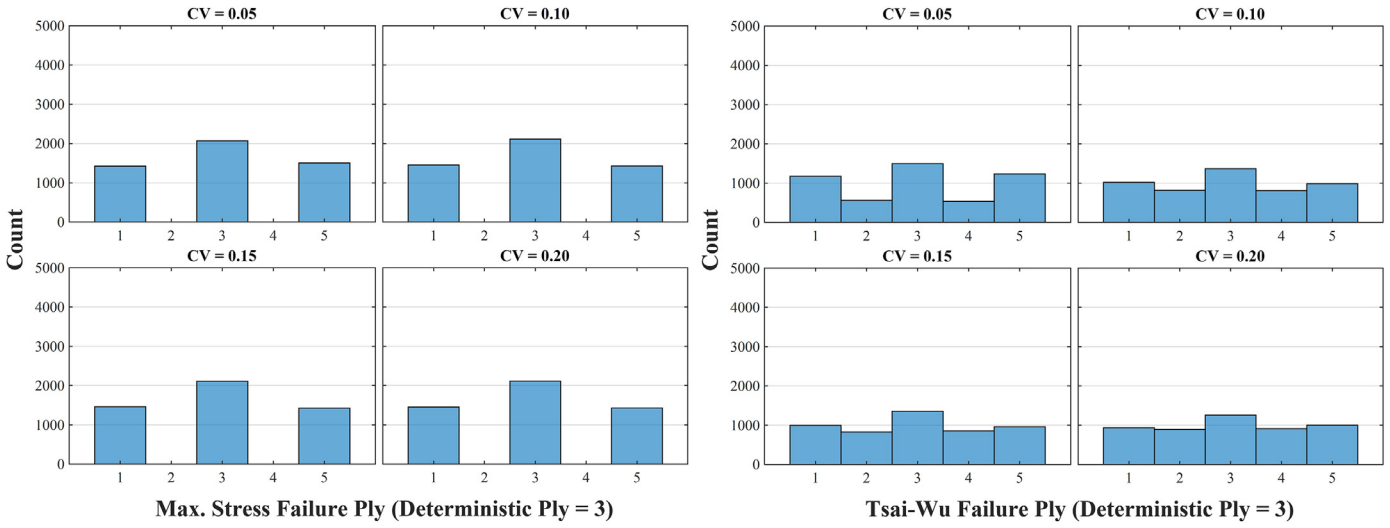

Fig. 18. Failure ply distributions, Graphite/epoxy, Laminate 4.

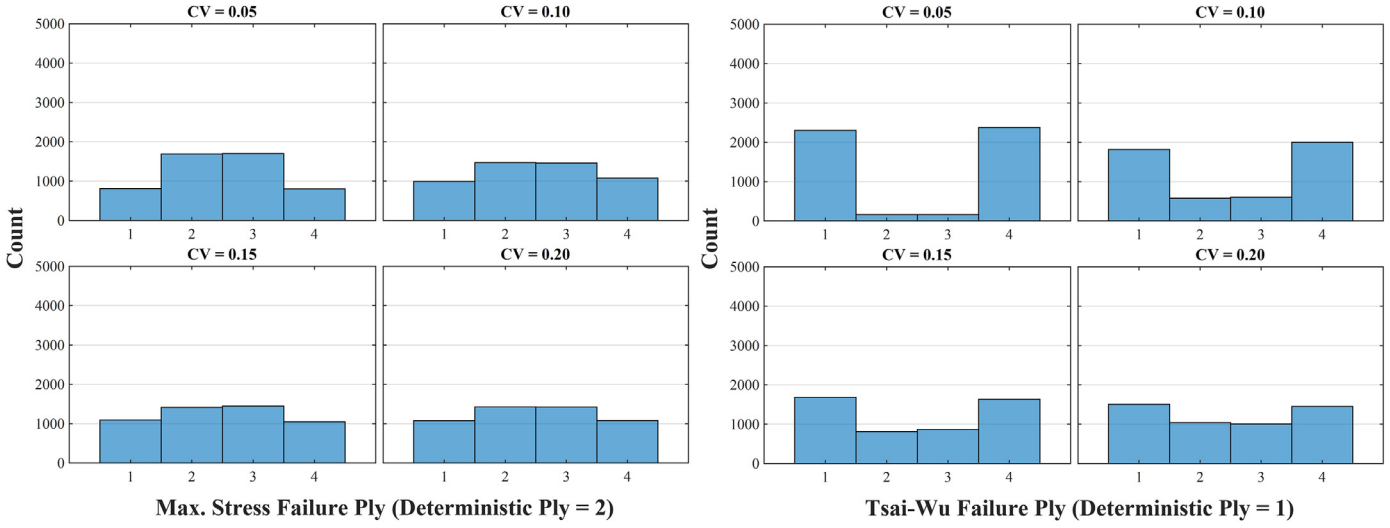

Fig. 19. Failure ply distributions, Graphite/epoxy, Laminate 5.

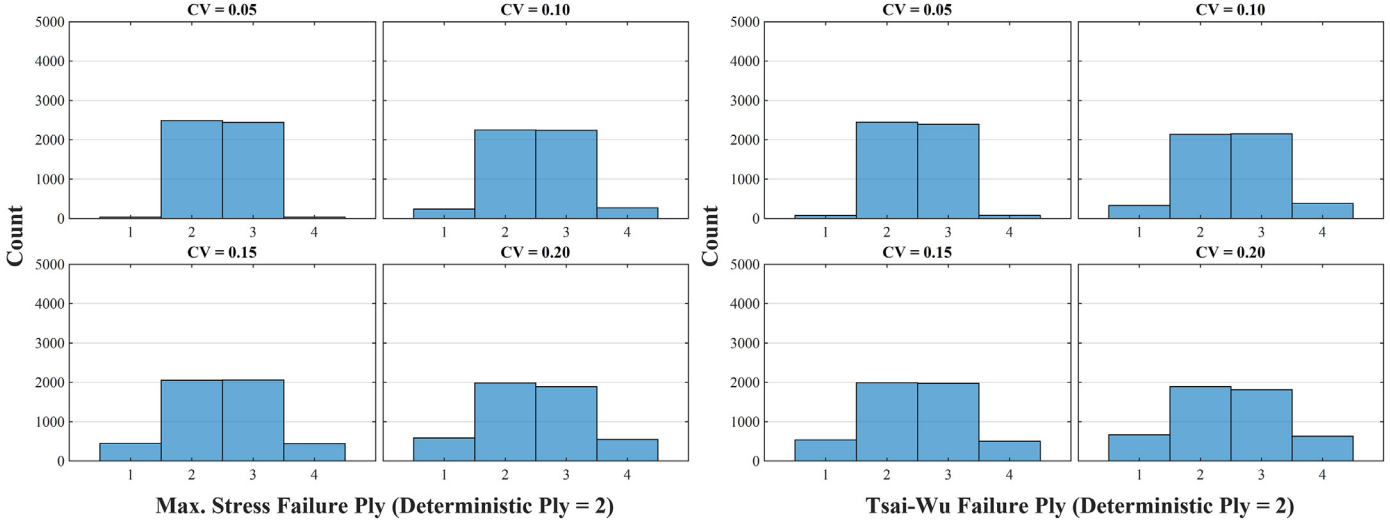

Fig. 20. Failure ply distributions, Glass/epoxy, Laminate 5.

Table 9
Median stiffness ratios (Max. Stress Failure Ply), Laminate 1.

Material	Failure Ply	g	$(E_1/E_2)_{Ply\ 2}$	$(E_1/E_2)_{Ply\ 3}$	$(E_1/E_2)_{Ply\ 5}$	$(E_1/E_2)_{Ply\ 6}$
Graphite/epoxy	2*	63.3%	**17.236**	17.797	17.612	17.605
	3	26.0%	18.774	**16.19**	17.767	17.647
	5	6.75%	19.332	18.968	**14.864**	17.954
	6	3.72%	19.568	18.989	18.459	**14.68**
Glass/epoxy	2*	59.0%	**4.5685**	4.7299	4.6851	4.6759
	3	27.7%	4.9511	**4.3143**	4.7266	4.6993
	5	8.33%	5.0688	4.9749	**4.0014**	4.7951
	6	5.00%	5.0655	5.0122	4.9115	**3.9261**
Boron/epoxy	2*	62.1%	**10.811**	11.173	11.051	11.047
	3	26.5%	11.773	**10.182**	11.155	11.104
	5	6.91%	12.125	11.885	**9.4052**	11.297
	6	3.81%	12.134	11.898	11.568	**9.1847**

* deterministic failure ply

Table 10
Median stiffness ratios (Max. Stress Failure Ply), Laminate 5.

Material	Failure Ply	g	$(E_1/E_2)_{Ply\ 1}$	$(E_1/E_2)_{Ply\ 2}$	$(E_1/E_2)_{Ply\ 3}$	$(E_1/E_2)_{Ply\ 4}$
Graphite/epoxy	1	17.8%	**16.407**	18.621	17.966	17.539
	2*	31.8%	17.904	**16.786**	17.828	17.603
	3	32.2%	17.611	17.815	**16.784**	17.911
	4	18.2%	17.609	17.959	18.655	**16.419**
Glass/epoxy	1	5.38%	**4.1323**	5.4336	5.0449	4.5788
	2*	44.6%	4.7356	**4.497**	4.7798	4.6338
	3	44.6%	4.6311	4.7746	**4.4977**	4.7353
	4	5.36%	4.5964	5.0377	5.4632	**4.1707**
Boron/epoxy	1	4.54%	**9.6411**	12.746	12.287	10.931
	2*	45.4%	11.155	**10.596**	11.347	10.972
	3	45.5%	10.969	11.332	**10.59**	11.151
	4	4.60%	10.963	12.29	12.722	**9.6632**

* deterministic failure ply

observations in plies 2 and 3. The same plot for glass/epoxy is almost inverted, with nearly all failures occurring in plies 2 and 3. This difference in behavior is likely related to the differences in the stiffness ratios for each material, whose deterministic values are 17.573, 4.667, and 11.027 for graphite/epoxy, glass/epoxy, and boron/epoxy, respectively.

The failure ply and median stiffness ratios (E_1/E_2) for laminates 1 and 5 can be found in Tables 9 and 10, which also provide the respective proportion of laminates through all 100,000 simulations in the third column as g, expressed as a percentage (i.e. g=count/100,000 × 100). These tables indicate that the median stiffness ratio is always lowest for the corresponding failed ply. Additionally, the median stiffness ratios for the cross-ply laminate (laminate 1) are higher in every instance where the failed ply changes. For example, for graphite/epoxy, in scenarios where ply 3 fails instead of the deterministic ply 2, the median stiffness ratio of ply 2 increased from 17.236 to 18.774, as shown in Table 9. In the less-common event that ply 5 fails, the median stiffness ratio of ply 2 increases further to 19.332. Moreover, the values of the median stiffness ratio for each scenario decreases with the likelihood of that particular ply failing (i.e., for graphite/epoxy failure plies 2, 3, 5, 6, whose empirical probabilities of failing are 0.63, 0.26, 0.068, and 0.037, the median stiffness ratios of the failure plies are 17.236, 16.190, 14.864, 14.680, respectively, as highlighted in bold in the table). A similar pattern is seen for laminate 5, though the overall behavior differs as shown in Fig. 20 and Table 10.

This suggests a sequential order to scenarios in which ply failures differ from the deterministic prediction; in order for a different ply to fail, not only must that ply have a lower stiffness ratio relative to the deterministic value, but the deterministic ply must simultaneously have a higher stiffness ratio. This also suggests that cross-ply laminates with failure plies different from what deterministic analysis predicts should accordingly have higher first-ply failure loads. This can be seen in Fig. 21, which shows a plot of laminate median $SR_{max.stress}$ for graphite/epoxy and glass/epoxy, grouped by the failure ply – each of the 4 lines in any plot represents an aggregate of the strength ratio for laminates with the failed plies designated by the legend. For example, the purple line in Fig. 21 shows, for any given CV(**X**), the median $SR_{max.stress}$ for laminates whose first failed ply is ply 6.

The deterministic failure ply (ply 2) has the lowest median strength ratio, followed by plies 3, 5, and 6. While laminates with failure plies other than the deterministic prediction do, in fact, correspond to higher strength ratios, it is worth reiterating that they are less likely to fail. This is particularly true for lower values of CV(**X**), as there is not enough variation in the input variables for a surprising outcome. For example, for laminate 1 of graphite/epoxy in Table 9, the deterministic ply fails in the majority (63.3%) of the total number of trials. This is also demonstrated in Fig. 21 for graphite/epoxy plies 5 and 6, for which no observations are seen for CV(**X**) less than 0.04. This pattern of sequentially increasing strength ratios is shown for both materials in Fig. 21, which is also reflected by the failure ply distribution in Fig. 17 (left).

Laminate 5 exhibits similar behavior, as shown in Fig. 22, which shows similar information as Fig. 21, but for Laminate 5. For graphite/epoxy, median strength ratios corresponding to the failure of plies 1 and 4 are indeed higher than the deterministic ply, but the difference is much less pronounced than for laminate 1. For ply 3, which is equally likely to fail as ply 2, there does not appear to be a significant difference. By comparing the graphite/epoxy plot in Fig. 22 (left) to the failure ply distributions in Fig. 19 (left) and empirical probabilities in Table 10, it can be seen that the differences in occurrence are less extreme than for laminate 1, which helps to explain why there is also a lesser difference between the strength ratios of different failure plies. Furthermore, unlike laminate 1, with which all materials had nearly identical failure ply distributions, laminate 5 glass/epoxy exhibits much different behavior between failure plies than graphite/epoxy. This behavior also mirrors the failure ply distributions shown in Fig. 20 – a more pronounced difference in the empirical probability results in a more pronounced increase in strength ratio. The different behavior in materials

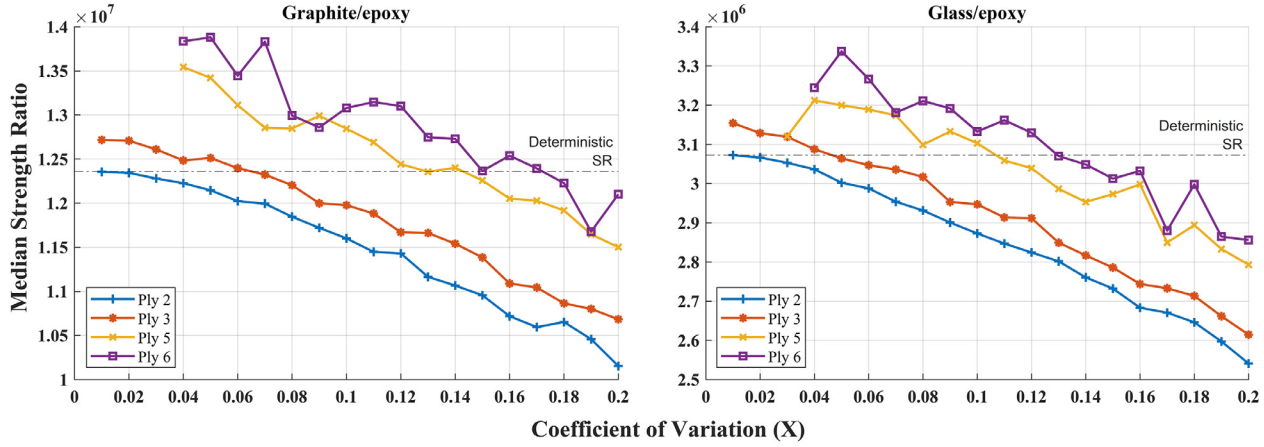

Fig. 21. Median $SR_{max.stress}$ by failed ply, Laminate 1.

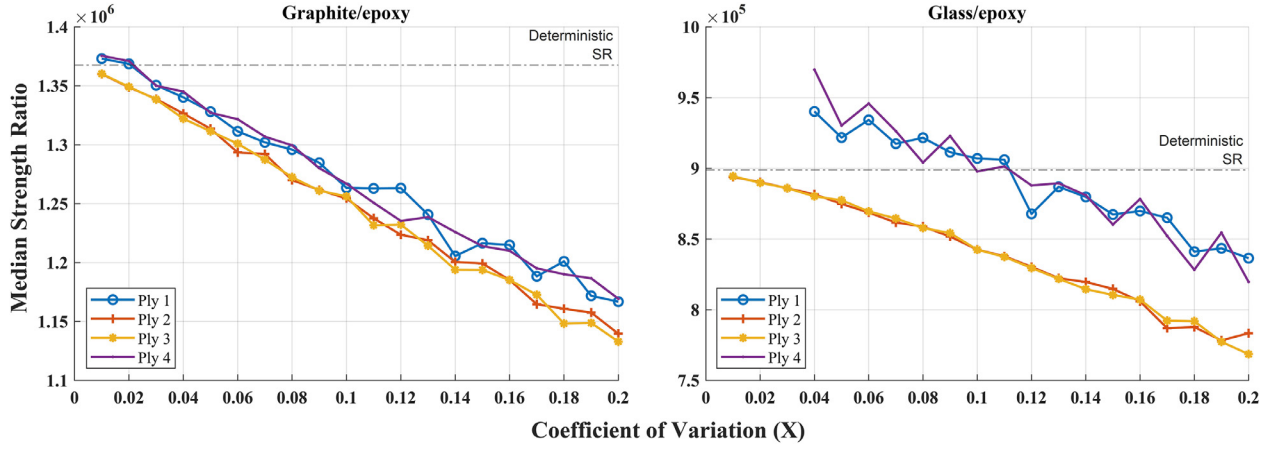

Fig. 22. Median $SR_{max.stress}$ by failed ply, Laminate 5.

is likely due to the innate difference in stiffness ratios between graphite and glass/epoxy as well as a difference in coupled behavior and stress distribution due to stacking sequence. The behavior exhibited by laminates 1 and 5 is not shared by laminates 2, 3, and 4, whose stiffness ratios are accordingly not shown. In fact, there does not appear to be any pattern in the stiffness ratios and the ply failures for these laminates, likely due to the contrast of coupling effects of the different laminate stacking sequences.

6. Conclusions

The stochastic effects on the response of composite laminated plates under static unidirectional tensile loading were investigated in this work by exploring the data generated via Monte Carlo simulation. The importance of considering randomness in the first-ply failure analysis of composite laminates is highlighted by the disproportionate response of coefficient of variation of strength ratio, CV(SR), to coefficient of variation of all material and geometric parameters, CV(**X**), with an emphasis on ply thickness and lamina strengths. Ply angle randomness is significant for balanced and angle-ply laminates, but not cross-ply and anti-symmetric laminates. A linear relationship between coefficient of variation of all input variables and both the strength ratio coefficient of variation and mean correction factor is demonstrated. The slope of the linear relationship is highly dependent on the combination of stacking sequence, material, and failure theory. Probability of failure is generally nonlinear, and no failure theory was found to always return the most or least conservative value. In general, there is an increasingly large penalty paid to ensure that a laminate meets the expected deterministic strength ratio, and this penalty increases with CV(**X**).

Failure plies predicted by deterministic analysis are often inaccurate when considering randomness in material properties and laminate parameters, though this accuracy is dependent on stacking sequence. For symmetric and antis-symmetric laminates, failure ply distributions reveal that the empirical probability of occurrence is virtually equivalent for both the deterministic ply and the opposite ply about the midplane of the laminate. In the case of cross-ply and anti-symmetric laminates, the failed ply has the lowest stiffness ratio. For cross-ply laminates in particular, there appears to be a sequential order to unexpected ply failures, which ultimately correspond to a higher first-ply failure load.

This paper demonstrated the nonlinearity of probability of failure of composite laminates, and the dependence of failure ply on the randomness of the laminate's material and geometric parameters. Divergence from deterministic, or expected, failure ply may or may not necessarily affect the strength ratio in a positive way. These findings underscore the importance of considering randomness in every available factor of the design of composite laminates: stacking sequence, material selection, and failure theory selection, among others. A few natural extensions of this research include, but are not limited to, the application of shear deformation theory, the consideration of hygrothermal effects, out-of-plane loading, and employing the full discount method to analyze behavior beyond first-ply failure. These extensions will be the subject of subsequent research.

Declaration of Competing Interest

The authors declare no conflict of interest.

Acknowledgements

The authors acknowledge the Department of Mechanical Engineering at California State University, Northridge. This research did not receive any specific grant from funding agencies in the public, commercial, or not-for-profit sectors.

References

[1] GS Ramtekkar, YM Desai, AH. Shah, First ply failure of laminated composite plates - a mixed finite element approach, J. Reinf. Plast. Compos. (2004), doi:10.1177/0731684404031464.
[2] N. Rattanawangcharoen, First-ply failure analysis of laminated composite cylindrical panels, J. Reinf. Plast. Compos. (2005) 10.1177/0731684405051657.
[3] BG Prusty, C Ray, SK. Satsangi, First ply failure analysis of stiffened panels - a finite element approach, Compos. Struct. (2001), doi:10.1016/S0263-8223(00)00126-4.
[4] BG Prusty, SK Satsangi, C. Ray, First ply failure analysis of laminated panels under transverse loading, J. Reinf. Plast. Compos. (2001), doi:10.1106/N050-RTTR-72JC-QJMB.
[5] P Pal, C. Ray, Progressive failure analysis of laminated composite plates by finite element method, J. Reinf. Plast. Compos. (2002), doi:10.1177/0731684402021016488.
[6] DJ Lekou, TP. Philippidis, Mechanical property variability in FRP laminates and its effect on failure prediction, Compos. Part B Eng. 39 (2008) 1247–1256, doi:10.1016/j.compositesb.2008.01.004.
[7] Z Maekawa, H Hamada, A Yokoyama, K Lee, S. Ishibashi, Reliability evaluation on mechanical characteristics of CFRP, Mech. Behav. Mat. VI (1992), doi:10.1016/b978-0-08-037890-9.50114-9.
[8] S Zhang, C Zhang, X. Chen, Effect of statistical correlation between ply mechanical properties on reliability of fibre reinforced plastic composite structures, J. Compos. Mater. (2015), doi:10.1177/0021998314558098.
[9] L Zhang, S Zhang, Y Jiang, J Tao, X. Chen, Compressive behaviour of fibre reinforced plastic with random fibre packing and a region of fibre waviness, J. Reinf. Plast. Compos. (2017), doi:10.1177/0731684416674070.
[10] S Sriramula, MK. Chryssanthopoulos, An experimental characterisation of spatial variability in GFRP composite panels, Struct. Saf. (2013), doi:10.1016/j.strusafe.2013.01.002.
[11] A Wagih, P Maimi, N Blanco, SM Garcia-Rodriguez, G Guillamet, RP Issac, A Turon, J. Costa, Improving damage resistance and load capacity of thin-ply laminates using ply clustering and small mismatch angles, Compos. Part A 117 (2019) 76–91.
[12] TA Sebaey, A. Wagih, Flexural properties of notched carbon–aramid hybrid composite laminates, J. Compos. Mater. 53 (28-30) (2019) 4137–4148.
[13] A Wagih, TA Sebaey, A Yudhanto, G. Lubineau, Post-impact flexural behavior of carbon-aramid/epoxy hybrid composites, Compos. Struct. 239 (2020) 112022.
[14] S Salim, D Yadav, NGR. Iyengar, Analysis of composite plates with random material characteristics, Mech. Res. Commun. (1993), doi:10.1016/0093-6413(93)90031-I.
[15] SC Lin, TY Kam, KH. Chu, Evaluation of buckling and first-ply failure probabilities of composite laminates, Int. J. Solids Struct. 35 (13) (1998) 1395–1410, doi:10.1016/S0020-7683(97)00113-3.
[16] W Wu, H Cheng, C. Kang, Random field formulation of composite laminates, Compos. Struct. 49 (2000) 87–93, doi:10.1016/S0263-8223(99)00128-2.
[17] AK Onkar, CS Upadhyay, D. Yadav, Probabilistic failure of laminated composite plates using the stochastic finite element method, Compos. Struct. 77 (1) (2007) 79–91, doi:10.1016/j.compstruct.2005.06.006.
[18] G Cederbaum, I Elishakoff, L. Librescu, Reliability of laminated plates via the first-order second moment method, Compos. Struct. 15 (1990) 161–167, doi:10.1016/0263-8223(90)90005-Y.
[19] TY Kam, SC Lin, KM. Hsiao, Reliability analysis of nonlinear laminated composite plate structures, Compos. Struct. (1993), doi:10.1016/0263-8223(93)90198-Y.
[20] TY Kam, ES. Chang, Reliability formulation for composite laminates subjected to first-ply failure, Compos. Struct. (1997), doi:10.1016/S0263-8223(97)00079-2.
[21] PD Gosling, Polit O Faimun, A high-fidelity first-order reliability analysis for shear deformable laminated composite plates, Compos. Struct. 115 (2014) 12–28, doi:10.1016/j.compstruct.2014.04.007.
[22] ME Tawfik, PL Bishay, EE. Sadek, Neural network-based second order reliability method (NNBSORM) for laminated composite plates in free vibration, Comput. Model. Eng. Sci. 115 (2018) 105–129, doi:10.3970/cmes.2018.115.105.
[23] RM. Jones, in: Mechanics of Composite Materials, 2nd ed., Taylor & Francis, London, 1999, p. 149, doi:10.1007/BF00611782.
[24] AK. Kaw, in: Mechanics of Composite Materials, 2nd ed., CRC Press, 2005, pp. 139–155. ISBN-13: 978-084931343.
[25] Wasserman, All of statistics : a concise course in statistical inference brief contents, Simulation (2004) 97–102, doi:10.1007/978-0-387-21736-9.
[26] S Gohari, S Sharifi, Z Vrcelj, MY. Yahya, First-ply failure prediction of an unsymmetrical laminated ellipsoidal woven GFRP composite shell with incorporated surface-bounded sensors and internally pressurized, Compos. Part B 77 (2015) 502–518, doi:10.1016/j.compositesb.2015.03.058.
[27] JN Reddy, AK. Pandey, A first-ply failure analysis of composite laminates, Comput. Struct. (1987), doi:10.1016/0045-7949(87)90130-1.
[28] RH Lopez, MA Luersen, ES. Cursi, Optimization of laminated composites considering different failure criteria, Compos. Part B 40 (2009) 731–740, doi:10.1016/j.compositesb.2009.05.007.
[29] UA Khashaba, TA Sebaey, KA. Alnefaie, Failure and reliability analysis of pinned-joints composite laminates: effects of stacking sequences, Compos. Part B 45 (2013) 1694–1703, doi:10.1016/j.compositesb.2012.09.066.